J. Membr. Biol. 13, 323–352 (1973)

A Parallel Path Model for *Necturus* Proximal Tubule

Kenneth R. Spring

Department of Physiology, Yale University School of Medicine,
333 Cedar Street, New Haven, Connecticut 06510

Received 12 March 1973

Summary. A parallel path model based on the principles of nonequilibrium thermodynamics was developed for the *Necturus* proximal tubule. The cellular path was represented as a luminal membrane followed by an irreversible active NaCl transport system in the peritubular barrier. The shunt pathway was described as three "coarse" barriers in series: tight junction, lateral intercellular spaces, and basement membrane with connective tissue. Volume and solute flows were predicted by the model equations as a function of applied electric current. Variations of the model parameters revealed the quantitative importance of the shunt path properties and the relative insensitivity of epithelial transport to changes in most cell parameters. Circulation of electric current and solute within the epithelium were shown to significantly influence the bahavior of the tubule in the presence of an electric field. Values for all transport parameters of the shunt path and epithelium were calculated and compared with available experimental evidence. Volume flow and electric currents predicted by the model compared favorably with experimental observations.

A new model for the renal proximal tubule is presented in an attempt to explain the results of the preceeding paper [34]. The proximal tubule is represented as a parallel path system in which one path (the extracellular) is composed of barriers in series. Previous investigators have suggested the possibility of fluid and ion flows through the tight junctions and extracellular shunt path. Bentzel *et al.* [8] proposed a tight junction path in parallel with the cell luminal membrane on the basis of fluid conductance and anatomical measurements. Boulpaep [11] put forth an analogous concept for ion permeation based on electrical measurements of the relative resistance of the epithelium and individual cell membranes. Many authors have since emphasized the importance of the extracellular shunt path in determining epithelial properties [13, 18–20, 29, 31, 45]. Models for such a parallel path system in the rat ileum [14] and gallbladder [3] were not in a form in which my results could be evaluated. The model presented here is a specific application of the

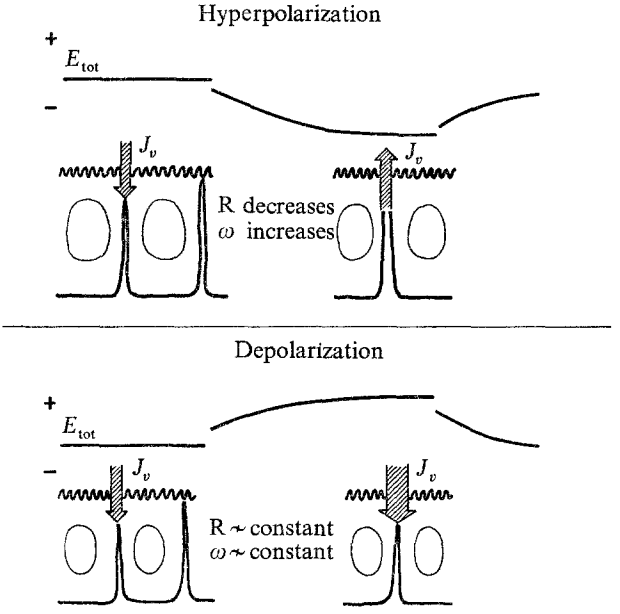

Fig. 1. Schematic representation of the changes in potential E_{tot}, volume flow J_v, resistance R, and salt permeability ω, that accompany the passage of a constant current stimulus. In the top half of the figure, current is passed which hyperpolarizes the tubule lumen with the result that J_v reverses, R decreases and ω increases. In the bottom half, current passage which depolarizes the tubule lumen increases J_v but does not significantly change R or ω

general nonequilibrium thermodynamic theory for multimembrane systems [28] to renal proximal tubule on the principle assumption that the tight junction-laterobasilar intercellular space path is in parallel with the tubule cells.

The purpose of this work is the duplication of the preceeding experimental observations by the use of a model system consistent with all known parameter values for *Necturus* proximal tubule. The experimental variables which were reproduced by the theoretical calculations are as follows: 1) E_{spon}, spontaneous PD; 2) E_{tot}, total PD; 3) I, electric current density; 4) J_v, volume flow. The equations also gave values for salt flow J_s which has not as yet been measured during current passage but may be assumed to match the volume flow to maintain luminal isotonicity. The general pattern of voltage transients and volume flows during current passage, described in the previous paper is recapitulated in Fig. 1. Also shown in that figure are the postulated changes in lateral intercellular space width which are correlated with changes in electrical resistance R and salt permeability ω. The parallel path equations adequately reproduced the individual results when supplied only with the initial values of E_{spon} and I and the continuous record of changes

in resistance. Reasonable representative values of all other parameters in the system were used to fit the experimental results. After the successful utilization of the equations to regenerate the experiments, variation of parameter values was undertaken to determine the critical variables in the epithelial model. A potential range of error in the measured values of most cell parameters had negligibly small effects on the volume or solute flows predicted by the model. Shunt parameter values were the major determinants of epithelial properties and the flows of salt and volume. Finally, estimates of the transport parameters of all significant components of the epithelium were made and used for further calculations and suggestions for future experimental design.

Theory

There are three passive flows in this parallel path system: volume flow J_v, solute flow J_s, and electric current I. The influence and mathematical representation of active transport will be discussed after formulation of the expressions for passive properties. The phenomenological equations which follow assume that flows of one salt (NaCl) constitute the only important solute movement, that the system is near equilibrium, and that flows are linearly related to forces.

$$I=\kappa\beta(\Delta P-\Delta\pi)+\kappa(t^+/\nu zF)\Delta\mu_s^c+\kappa E, \tag{1}$$

$$J_v=Lp(\Delta P-\Delta\pi_i)-\sigma Lp\Delta\pi_s+\beta I, \tag{2}$$

$$J_s=\bar{C}_s Lp(1-\sigma)(\Delta P-\Delta\pi)+\omega\Delta\pi_s+(t^+/\nu zF)I \tag{3}$$

where:

Parameters

κ = electrical conductance, mho/cm^2

β = electroosmotic coupling coefficient, cm^3/coul

t^+ = cation transference number

ν = stoichiometric coefficient

z = cation valence

F = Faraday

Lp = hydraulic conductivity, cm^3/dyne sec

σ = solute reflection coefficient

$\bar{C}_s$ = average concentration in epithelium, M/cm^3

ω = solute permeability coefficient, mole/dyne sec.

Flows

I = electric current, amp/cm^2

J_v = volume flow, cm/sec

J_s = solute flow, moles/cm^2 sec

Forces

ΔP = hydrostatic pressure difference, dynes/cm^2

$\Delta \pi_i$ = osmotic pressure due to impermeant solute, dynes/cm^2

$\Delta \pi_s$ = osmotic pressure due to permeant solute (NaCl), dynes/cm^2

$\Delta \pi = \Delta \pi_i + \Delta \pi_s$

$\Delta \mu_s^c = \Delta \pi_s / \bar{C}_s$ (special definition for these equations), dyne cm/mole

E = electromotive force of epithelium, volts.

All flows and forces are defined as ECF-lumen so that a positive J_v represents droplet swelling and would be the consequence of a negative $\Delta \pi$ (e.g., higher π in lumen than ECF). NaCl is treated as an electroneutral component which dissociates into equal numbers of cations and anions. Treatment of solute movements as the flow of neutral salt results in a simplified representation from which we can gain a comprehensible overview of the mechanisms of proximal tubular fluid transport. This model can be expanded to include ionic flows if the experimental observations are made which justify the additional complexity and furnish the requisite new data. The potential difference (PD) measured experimentally may, under the conditions of these experiments, be equated with E with negligible error.

In Eq. (1), electric current is the sum of three current flows: the first due to electroosmotic coupling, the second to ion permeation and the last to potential drop across the epithelial resistance. J_v in Eq. (2) is also composed of three components: 1) hydrostatic-oncotic forces, 2) permeant solute osmotic pressure, and 3) electroosmosis. J_s in Eq. (3) is the sum of: 1) solvent drag, 2) concentration dependent diffusional flux, and 3) ion permeation caused by electric current flow.

The derivation of these equations assumes that the electrodes used for the passage of current and measurement of PD are completely anion reversible. Since this situation does not apply to any experiments to date on renal proximal tubule for either current passage or voltage measurements, it was necessary to reformulate the equations for this particular case. If the current electrodes are nonreversible the expression for the cation transference number (t^+) in Eqs. (1) and (3) must be replaced by the difference between cation and anion transference numbers ($t^+ - t^-$), henceforth denoted as t_D [26]. This alteration comes about simply because the reversible electrodes were assumed

in the original derivation to take up or give off chloride in sufficient amounts to eliminate consideration of its flow through the membrane.

At this point it is worthwhile to consider the influence of active transport processes on the form of the phenomenological equations. Hoshiko and Lindley [24] incorporated active transport into Eqs. (1)–(3) and found the following results: Eq. (1) for electric current had an additional term εJ_r representing the coupling of current to active transport; Eq. (2) had an additional term VJ_r representing the coupling of volume flow to active transport; Eq. (3) had another term UJ_r for the coupling of solute flow to active transport. An additional phenomenological equation defined J_r, the metabolic flow rate, in terms of the other flows and forces multiplied by their appropriate coupling coefficients. While these equations are thermodynamically correct in their representations of the influences of active transport, they seriously complicate the analysis by the inclusion of five more parameters and another phenomenological equation. Representation of the proximal tubule as a transport system involving both NaCl and KCl increases the number of phenomenological equations to five and results in a total of 12 to 15 parameters which must be determined experimentally. Most of these coupling parameters have not or cannot be determined experimentally in the proximal tubule. I chose, therefore, to formulate a model assuming that active transport does not significantly influence the parameter estimates or alter during the passage of electric current. It is assumed that diffusion into the cell is exactly equalled by active transport out of it, and that cell composition is unchanged during current passage. As shown in Fig. 6 of the preceeding paper and by Boulpaep [12], the fraction of electric current passing through the cell is very small, and any alterations in cellular composition which could result from such a current are probably compensated for by the Na-K exchange pump or by active extrusion of NaCl.[1] The influence of active transport on the estimates of tubular permeability and hydraulic conductivity is unknown. As shown by Jacquez *et al.* [25] and Hoshiko & Lindley [24], possible coupling or reversibility of the pump significantly alters the values of permeability, hydraulic conductivity and the coupling coefficients for transport. Since these possible effects have not been investi-

1 The magnitude of the alteration in the normal influx of NaCl due to diffusion into the cell during current passage was calculated with the least favorable estimates of the transference numbers for the luminal and peritubular membranes. Neglecting active Na-K exchange, continuous passage of 10^{-4} amp/cm^2 leads to an eventual increase in intracellular NaCl of about 8 mM/liter and an equal depletion of KCl. A 25% change in passive ionic influx of NaCl would occur during current passage. Since these effects are being opposed by active NaCl extrusion and Na-K exchange, I assume them to be of minor importance in determining the characteristics of the epithelium.

gated in proximal tubule, they cannot be realistically incorporated into the model at this time.

Each of the parameters in Eqs. (1)–(3) may be defined for a parallel path system as the weighted sum of the individual values for cell and shunt paths, respectively [28]. A cross or interactive term often enters into the calculations and is indicated where applicable. The method of application of the following equations is eminently simple and direct – if one knows the value of a parameter for the entire system and for one of the paths (cell or shunt) then it is possible to calculate the properties of the other path by subtraction.

Total epithelial solute permeability ω is defined by:

$$\omega = \gamma_a \omega_a + \gamma_b \omega_b + \frac{(t_D^a - t_D^b)^2 \alpha_a \alpha_b \kappa}{\bar{C}_s (\nu z F)^2} \tag{4}$$

where a refers to the cellular path and b to the shunt path, γ is the fraction of total area occupied by each path, α the fraction of electric current in each path, and the remaining symbols are previously defined.

Total transference number difference t_D is defined by:

$$t_D = \alpha_a t_D^a + \alpha_b t_D^b. \tag{5}$$

Electroosmotic coupling coefficient β by:

$$\beta = \alpha_a \beta_a + \alpha_b \beta_b. \tag{6}$$

Electrical conductance κ by:

$$\kappa = \alpha_a \kappa_a + \alpha_b \kappa_b. \tag{7}$$

Hydraulic conductivity Lp by:

$$Lp = \gamma_a Lp_a + \gamma_b Lp_b + \alpha_a \alpha_b \kappa (\beta_a - \beta_b)^2. \tag{8}$$

Solute reflection coefficient σ by:

$$1 - \sigma = \gamma_a (1 - \sigma_a) \frac{Lp_a}{Lp} + \gamma_b (1 - \sigma_b) \frac{Lp_b}{Lp} + \frac{\alpha_a \alpha_b \kappa (\beta_a - \beta_b)(t_D^a - t_D^b)}{\nu z F \bar{C}_s Lp}. \tag{9}$$

It may be generally seen that electrical parameters t_D, κ, β add linearly and are weighted by the fraction of electric current α through each path. Solute and fluid parameters, on the other hand, all exhibit nonlinear summation and are weighted according to their area fraction γ.

Epithelial Parameters

The epithelial parameters of the *Necturus* proximal tubule which have been determined experimentally are listed in the first column of Table 1 together with the values for the tubule cells and shunt path measured or calculated as described below.

Table 1. Transport Parameters of Proximal tubule

Parameter	Total epithelium	Tubule cell	Shunt path
ω-NaCl permeability mole/dyne sec	$1 \rightarrow 2.8 \times 10^{-16}$ (1)	$0.35 \rightarrow 0.74 \times 10^{-16}$ (2)	1.3×10^{-16} [a]
σ-NaCl reflection coefficient	0.69 (3)	0.97 (2)	0.67[a] (0.13) (11)
Lp-Hydraulic cond. cm^3/dyne sec	0.33×10^{-11} (4)	0.28×10^{-12} (2)	0.27×10^{-11}[a]
t_{Na}-transference no.	0.40 (5)	$0.5 \rightarrow 0.65$ (6)	0.385[a] (0.52)[b]
κ-conductance mho/cm^2	$14.3 \rightarrow 25 \times 10^{-3}$ (7)	$0.23 \rightarrow 2.8 \times 10^{-3}$ (8)	$15 \rightarrow 22 \times 10^{-3}$[a]
γ-area fraction/cm^2	1	0.9997 (9)	2.7×10^{-4} (9)
β-Electroosmotic coupling cm^3/coul	$\simeq 0$ (5)	0.11×10^{-2} (10)	$\simeq 0$[a]

References

1. [13, 35, 41].
2. [41].
3. [7].
4. [7, 8].
5. E. L. Boulpaep, *unpublished observation.*
6. Estimated from data of Boulpaep [12].
7. [13, 34, 35].
8. Estimated range as described in text.
9. Calculated from dimensions of tight junction given in text, assumes smooth luminal surface.
10. Calculated from cell pore size of 5 Å [40].
11. σ of 0.67 represents tight junction only, 0.13 is effective σ calculated from Eq. (12) as described in text.

[a] Calculated from the parallel path Eqs. (4–9).

[b] Estimated from fitting current clamp experiments (*see* text).

Cellular Path

Anatomically, the tubule cell consists of a highly infolded luminal membrane, somewhat tortuous lateral membranes and a slightly convoluted basal membrane. Electrophysiological evidence in *Necturus* indicates that the NaCl

permeability of the baso-lateral membranes is very small (1/10 or less) compared to that of the luminal membrane [12, 21]. Diffusion of NaCl into the cell across the peritubular membrane is considered to be negligible compared to the influx across the luminal membrane. The luminal membrane displays a greater electrical resistance than the peritubular [12, 43] and presumably a lower hydraulic conductivity than the peritubular membrane [8]. In the present model, the passive cellular properties were chosen to be those of the luminal membrane and the active component an irreversible Na pump at the peritubular border.

A number of parameters of the proximal tubule cell of *Necturus* kidney have been measured and are listed in Table 1. Two variables, the transference numbers for the luminal membrane, and the exact value of its electrical resistance are not known with certainty. An estimate of the transference numbers may be made from the data of Boulpaep [12] which can be used to calculate a t_{Na} of $0.5 \rightarrow 0.65$. Luminal membrane resistance was reported by Windhager *et al.* [43] as about $4500\ \Omega\ cm^2$ but consideration of the area assumptions may result in a resistance as low as $350\ \Omega\ cm^2$. It will be seen subsequently that such a range of possible values for the luminal membrane resistance has virtually no influence on the volume flows predicted by the model.

Shunt Path

Although I have effectively reduced the cellular path to a single passive barrier this is not possible in the shunt path. As discussed in the first paper of this pair, the shunt is composed of three "barriers" in series: tight junction (*TJ*), lateral intercellular spaces (*Lis*), and basement membrane with associated connective tissue (*bm*). The overall properties of a series membrane system are described by the following equations [28].

Total permeability to solute ω_b is given by:

$$\frac{1}{\omega_b} = \frac{1}{\gamma_{TJ}\,\omega_{TJ}} + \frac{1}{\gamma_{Lis}\,\omega_{Lis}} + \frac{1}{\gamma_{bm}\,\omega_{bm}}. \tag{10}$$

where the ω_i are the respective solute conductances of each barrier; γ_i are the relative areas of each barrier.

Total shunt transference number difference t_D^b:

$$t_D^b = t_D^{TJ}\left(\frac{\omega_b}{\omega_{TJ}}\right) + t_D^{Lis}\left(\frac{\omega_b}{\omega_{Lis}}\right) + t_D^{bm}\left(\frac{\omega_b}{\omega_{bm}}\right) \tag{11}$$

where $t_D^i = (t^+ - t^-)_i$ for each barrier.

Effective solute reflection coefficient σ_b:

$$\sigma_b = \sigma_{TJ}\left(\frac{\omega_b}{\omega_{TJ}}\right) + \sigma_{Lis}\left(\frac{\omega_b}{\omega_{Lis}}\right) + \sigma_{bm}\left(\frac{\omega_b}{\omega_{bm}}\right). \tag{12}$$

Hydraulic conductivity Lp_b equals:

$$\frac{1}{Lp_b} = \frac{1}{\gamma_{TJ} Lp_{TJ}} + \frac{1}{\gamma_{bm} Lp_{bm}} + \frac{\bar{C}_s(\sigma_{TJ} - \sigma_{bm})^2}{\omega_{TJ} + \omega_{Lis}} \tag{13}$$

where $\bar{C}_s$ is the average solute concentration in the middle compartment, $\bar{C}_s = C' - C''/\ln(C'/C'')$.

Electrical conductance κ_b:

$$\frac{1}{\kappa_b} = \frac{1}{\kappa_{TJ}} + \frac{1}{\kappa_{bm}} + \frac{(t_D^{TJ} - t_D^{Lis})^2}{\bar{C}_s(\nu z F)^2(\omega_{TJ} + \omega_{Lis})}. \tag{14}$$

Electroosmotic coupling coefficient β_b:

$$\beta_b = \beta_{TJ}\left(\frac{Lp_b}{Lp_{TJ}\gamma_{TJ}}\right) + \beta_{bm}\left(\frac{Lp_b}{Lp_{bm}\gamma_{bm}}\right) + \frac{Lp_b(\sigma_{TJ} - \sigma_{bm})(t_D^{TJ} - t_D^{bm})}{\nu z F(\omega_{TJ} + \omega_{Lis})}. \tag{15}$$

When electric current is passed through a series membrane system, salt may be accumulated or depleted in the space between the barriers. If we consider a thin layer of solution adjacent to the tight junction and separated from the ECF by the remaining lateral space and basement membrane, the osmotic pressure of the change in solute concentration caused by current passage is given by:[2]

$$\Delta\pi_s = \frac{(t_D^{Lis} - t_D^{TJ})I}{\nu z F(\omega_{TJ} + \omega_{Lis})}. \tag{16}$$

This osmotic pressure increase is equivalent to a concentration increase of NaCl by Vant Hoff's Law:

$$\Delta\pi_s = RT\Delta C_s \tag{17}$$

2 This expression, from Kedem and Katchalsky [28], is similar in form to the equation for the transport number effect presented by Barry and Hope [4]. Eq. (16) includes both the buildup of concentration due to transport number discontinuity and its principal dissipation from diffusion of solute across the tight junction and into the lateral space. Barry and Hope also included dissipation due to sweeping away of solute by volume flow (neglected here since the maximal effect is on the order of 10% of the concentration change caused by current passage) and diffusion of solute away from the interface back into bulk solution. I have assumed that such diffusion occurs at the luminal surface and eliminates the need for consideration of concentration changes at that surface.

where R is the gas constant, T the absolute temperature, and ΔC_s the resultant concentration difference. Such a concentration difference across the shunt path results in an EMF according to the following equation derived in the appendix:

$$\Delta E=(t_D^{Lis}-t_D^{TJ})\frac{RT}{\nu zF}\ln\frac{C+\Delta C_s}{C} \tag{18}$$

where C is the concentration of NaCl in the absence of current passage.

These three equations, (16)–(18), form the theoretical basis for the relationship between applied electric current, volume flow and voltage transient. Current passage leads to salt accumulation or depletion [Eq. (16)] which results in both a transepithelial PD change [Eqs. (17) and (18)] and a volume flow [Eq. (2)]. I will now consider the properties of each portion of the shunt path of the *Necturus* proximal tubule.

Basement Membrane and Associated Connective Tissue

This portion consists of a loose bed of connective tissue adjacent to an amorphous basement membrane (about 1 μm thick) which has a total surface area 1.45 times greater than that of the lumen (assuming smooth surfaces for each). The effective thickness of this barrier may be estimated from the diffusional delay in peritubular depolarization upon perfusion of the peritubular capillaries with high concentrations of KCl. A t 1/2 of 5 sec was reported by Asterita [2] which leads to an estimated tissue thickness of about 10 μm if the diffusion coefficient of KCl is identical to free solution. Effective NaCl permeability ($\gamma_{bm}\,\omega_{bm}$) may be calculated for such a "coarse" membrane by the formula given in Kedem and Katchalsky [27] (also, Eq. (9) of the preceeding paper) as about 1.0×10^{-12} mole/dyne sec, a value so low that the basement and connective tissue may be neglected as barriers to solute diffusion. A lower limit for the hydraulic conductivity of the basement membrane may be estimated from the hydrostatic pressure measurements of Grandchamp and Boulpaep [22]. The hydrostatic pressure drop between peritubular capillaries and tubule lumen probably occurs across the relatively rigid basement membrane [37] since the remaining tissue is deformable and cannot support large hydrostatic pressure differences. Assuming the principal barrier to hydrostatic pressure is at the basement membrane itself, I calculate that $Lp_{bm}\geqq0.377\times10^{-10}$ cm^3/dyne sec. The basement membrane is assumed to be penetrated by large pores ($\therefore\ \sigma_{bm}=0$), be uncharged ($\therefore\beta_{bm}=0$ and $t_{bm}^{D}=-0.23$, free solution value) and have high electrical conductivity ($\kappa_{bm}=72.5$ mho/cm^2 epithelium).

Lateral Intercellular Spaces

These are long, narrow paths winding from tight junction to basement membrane with the following approximate dimensions: linear length 800 cm/cm^2 epithelium [13], average width 0.2 μm [8], depth 25 μm [5, 38], tortuosity factor 2.3 [38], calculated cross-sectional area 1.6×10^{-2} cm^2/cm^2 epithelium. Effective NaCl permeability ($\gamma_{Lis}\ \omega_{Lis}$) for this space as a coarse membrane with diffusion of NaCl restricted to one-fifth of its free solution rate is 0.16×10^{-15} mole/dyne-sec. The lateral space would be expected to show no salt reflection ($\sigma_{Lis}=0$) and be uncharged ($\beta_{Lis}=0$ and $t_D^{Lis}=-0.23$, free solution value). The electrical conductance for such a Ringer's-filled space is about 0.026 mho/cm^2 epithelium and is directly proportional to its dimensions. The lateral space hydraulic conductivity is virtually that of free solution and does not enter into calculations involving Lp unless the space width is $\leq$ 100 Å [45].

Tight Junction

Tight junctions are extremely narrow clefts or slits surrounding cells at the luminal border with the following average dimensions: linear length 800 cm/cm^2 epithelium [13], slit width 25 to 34 Å [5, 8], depth 500 to 1 000 Å [5, 15], calculated cross-sectional area for a 34-Å slit width is 2.7×10^{-4} cm^2/cm^2 epithelium. Effective NaCl permeability ($\gamma_{TJ}\ \omega_{TJ}$) is 0.645×10^{-15} mole/dyne sec assuming a diffusion coefficient restricted to one-fifth of the free solution value in this "coarse" barrier. Its hydraulic conductivity, calculated from Eq. (15) is 0.10×10^{-7} cm^3/dyne sec, an order of magnitude smaller than a system of tortuous capillaries of similar dimensions. NaCl reflection coefficient is 0.667, calculated from Eq. (9) as described below. Electroosmotic coupling is negligible based on the absence of significant streaming potentials (E. L. Boulpaep, *unpublished observation*). The transference number difference is calculated to be 0.25 from Eqs. (16) and (18) by fitting to experimental data as described below. Electrical conductance for a Ringer's-filled tight junction is about 0.136 mho/cm^2 epithelium.

All of the above parameters are summarized in Table 2 where also included are the calculated properties of the entire shunt path. The published experimental values for σ and Lp of the tubule were assumed in the model to represent the parameters of the luminal cell membrane in parallel with the tight junctions only rather than those of the epithelium as a whole. This approach was used because measurements of epithelial properties such as permeability, solute reflection coefficient and hydraulic conductivity, from the instantaneous determination of volume or solute flows into or out of the tubule lumen (time zero extrapolation method) reflect primarily the prop-

Table 2. Shunt path parameters

Parameter	Tight junctions (*TJ*)	Lateral intercellular space (*Lis*)	Basement membrane (*bm*)	Calculated shunt path (*b*)
γ_i Cross-sectional area cm^2/cm^2 epithelium	2.7×10^{-4}	1.6×10^{-2}	1.45	2.7×10^{-4}
α_i Electric current fraction	$\simeq0.94$	$\simeq0.94\rightarrow1.0$	1.0	$\simeq0.94$
t^i_{Na} Na transference number	0.63→0.67	0.385	0.385	(0.52)[a] 0.41
Ω_i Electrical resistance ohm cm^2 epithelium	7.3	37.5→375	<0.01	≃45→55
σ_i NaCl reflection coefficient	0.667	0	0	0.13
$\omega_i\gamma_i$ Area adjusted NaCl permeability coefficient mole/dyne sec	0.65×10^{-15}	0.16×10^{-15}	1.07×10^{-12}	0.13×10^{-15}
$Lp_i\gamma_i$ Area adjusted hydraulic conductivity cm^3/dyne sec	0.28×10^{-11}	$\geq10\times10^{-7}$	$\geq0.38\times10^{-10}$	0.27×10^{-11}
β_i Electroosmotic coupling coefficient cm^3/coul	$\simeq0$	$\simeq0$	$\simeq0$	$\simeq0$

[a] Transference number estimated from current clamp experiments.

erties of the barrier closest to the tubule lumen (i.e., the cell luminal membrane and tight junction in parallel). This point was emphasized by Bentzel *et al.* [7] in their determination of reflection coefficients and hydraulic conductivity [8], and by Solomon [33] in his analogue model of the results of Oken *et al.* [30].

NaCl Reflection Coefficient

The reflection coefficient for NaCl of the tubule epithelium was estimated as 0.69 by the time zero extrapolation method [7]. Since the reflection coefficient for the cellular path is 0.97 [38, 41], the shunt estimate would be expected to be considerably less than 0.69. The reflection coefficient of only the tight junction and that of the cell were used in Eq. (9) to obtain the value measured experimentally. The effective steady-state NaCl reflection coefficient of the shunt path is considerably lower (Table 2) when calculated from Eq. (12).

Hydraulic Conductivity

Lp measured from the luminal volume changes induced by osmotic pressure differences reflects primarily the properties of the tight junction and luminal cell membrane in parallel. Two factors are involved: first, the time zero extrapolation method [7, 8] gives the *Lp* of only the luminal barrier; and secondly the reflection coefficient of the basement membrane is ≈ 0 for NaCl. An osmotic gradient of NaCl cannot exist across the basement membrane of the *Necturus*. This is supported by experimental evidence demonstrating the rapid passage of large molecular weight substances, such as horseradish peroxidase, through the basement membrane and into the lateral spaces of the epithelium of the proximal tubule [10]. Finally, the *Lp* of the shunt is nearly equal to that of the tight junction since $\gamma_{bm} Lp_{bm}$ it at least 10 times greater than $\gamma_{TJ} Lp_{TJ}$.

Transference Number Difference

Although no published data are available concerning the transepithelial transference numbers of *Necturus* proximal tubule, Dr. Boulpaep was kind enough to make unpublished observations available. He determined the transepithelial transference numbers for Na and Cl by perfusing the tubule lumen with low concentrations of NaCl and observing the magnitude and direction of the instantaneous change in transepithelial PD. When the epithelium is considered as a lumped, single barrier, the overall transference numbers obtained from these experiments agree with those in Table 1 and those calculated from Eq. (11). When the shunt parameters in Table 2 are inserted in Eq. (11), the principal determinants of the total transepithelial transference numbers are the transference numbers of the lateral intercellular spaces, which I have assumed to be near free solution values. Thus, during a salt dilution experiment the epithelium exhibits transference values near free solution; however, as described in the appendix to this paper, salt gradient experiments may be interpreted differently if a distributed parameter model of the epithelium (or shunt path) is employed. In the more complex treatment transference numbers estimated from salt gradients are a function of the concentration profiles within the epithelium during the experiment as well as the properties of the barriers themselves. From Eq. (7) of the Appendix, the approximate range of Na transference number of the tight junction, compatible with the experimental results of Boulpaep, is 0.40 to 0.70 depending on the NaCl concentration profile chosen to represent the situation within the shunt pathway. Application of the model equations to current clamp experiments requires a shunt Na transference number of about 0.52.

Table 3. Model parameters and forces used in Eqs. (1)–(3)

	Value	Source
Electrical conductance, κ	18×10^{-3} mho/cm^2	[34]
Electroosmotic coupling, β	0.11×10^{-2} cm^3/coul	Table 1
Transference number difference, t_D	0.065	Estimated from current clamp
Hydraulic conductivity, Lp	0.33×10^{-11} cm^3/dyne sec	Eq. (13), [7]
Reflection coefficient, σ	0.69	Eq. (9), [7]
Solute permeability, ω	0.15×10^{-15} mole/dyne sec	Eq. (4), [13, 35]
Hydrostatic pressure difference, ΔP	-3.3 cm H_2O	[22]
Oncotic pressure difference, $\Delta\pi_i$	9.3 cm H_2O	[22]

The data of Tables 1 and 2 were utilized in Eqs. (1)–(3) to predict the relationship between applied current and fluid movement. Calculations were performed on an IBM 370/155 digital computer. Two general approaches were used: first, parameters were held constant while the forces were systematically varied, or the forces were held constant and individual parameters altered over a reasonable range; second, after the optimal estimates of the parameters had been made, the voltage, current, volume and solute flows of individual current clamp experiments were duplicated. The normally obtaining parameters and forces, listed in Table 3, were not varied unless they were specifically the subject of investigation. The use of steady-state equations to duplicate transient phenomena was accomplished by computing a series of steady-state solutions during the transient. The equations were recomputed at short intervals and the transients generated incrementally.

The working equations were in the same form as Eqs. (1)–(3) with two exceptions. In Eq. (3) for J_s, the diffusional flux of NaCl ($\omega\Delta\pi_s$) was divided into its two major components: $\gamma_b\omega_b\Delta\pi_s$, diffusion into or out of the shunt path, and $\gamma_a\omega_a\Delta\pi_s^c$, diffusion into the cells across the luminal membrane. $\Delta\pi_s^c$ is the osmotic pressure difference due to the NaCl concentration gradient between cell interior and tubule lumen (cell $Na^+ = 37$ mM/liter, $Cl^- = 32$ mM/liter [41]). Passive influx into the cell is exactly matched by an active efflux into the baso-lateral spaces, which results in an additional term in Eq. (2) (J_v) for the volume flow caused by active transport. Since active NaCl movement in *Necturus* tubule is known to result in isosmotic fluid flux, the J_v due to transport was set equal to:

$$J_s^{\text{active}}/\bar{C}_s(1-\sigma_b) \tag{19}$$

where J_s^{active} is the amount of NaCl transport out of the cell and into the shunt (equal to $\gamma_a\omega_a\Delta\pi_s^c$).

Results

Fig. 2 shows the dependence of J_v and J_s as well as E on the applied electric current in a representative tubule. The parameter and variable values used to generate these curves are given in Table 1 (tubule cell), Table 2 (shunt) and Table 3 (total epithelial). Fluid flow is virtually isosmotic when these values are used and agrees well with the overall experimental results. The relative flows of solute and solvent through the cellular and shunt paths in the absence of applied electric current are of special interest. The volume flow through the cells is only 14% of the total when both paths are exposed to the same osmotic pressure gradient. Solute flows may be partitioned as shown in Fig. 3. Most of the net solute movement is attributable to active transport by the cells into the shunt path, while back flux due to the various factors outlined in Fig. 3 amounts to about 60% of active transport rate and results in an overall flux ratio (active/net flux) of 1.90.

Alterations in the physical driving forces $\Delta\pi_i$ and ΔP are nearly without effect on the rate of volume flow consequent to electric current passage. The osmotic pressure of impermeant solutes ($\Delta\pi_i$) was varied from 1 to 19 cm H_2O with no significant effect on J_v or J_s; alterations in ΔP from -8 to $+10$ cm H_2O were also ineffective. Several previous investigators [6, 39, 42] have suggested that these forces, per se, are insufficient to alter volume flow but may lead to significant changes if morphological alterations occur.

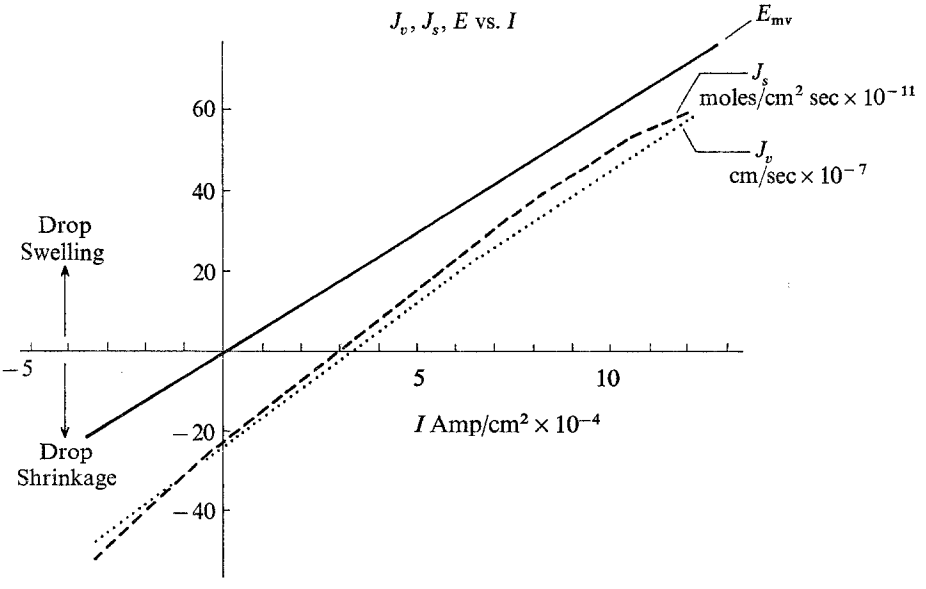

Fig. 2. Volume flow (J_v), solute flow (J_s) and transepithelial PD (E) on the ordinate are plotted as a function of the electric current (I) on the abscissa

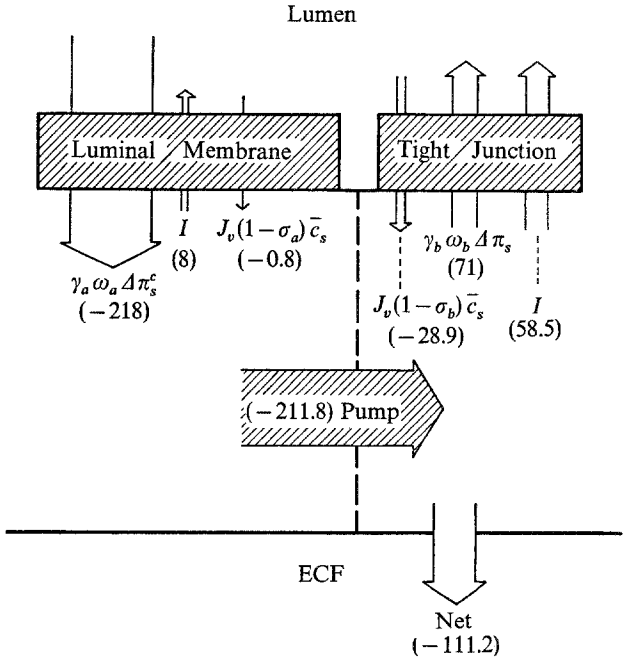

Fig. 3. Flows of NaCl in parallel path model due to diffusion ($\gamma\omega\Delta\pi_s$), electric current (I), solvent drag ($J_v(I-\sigma)\bar{C}_s$) and active transport (pump). All numerical values are in pmoles/cm² sec

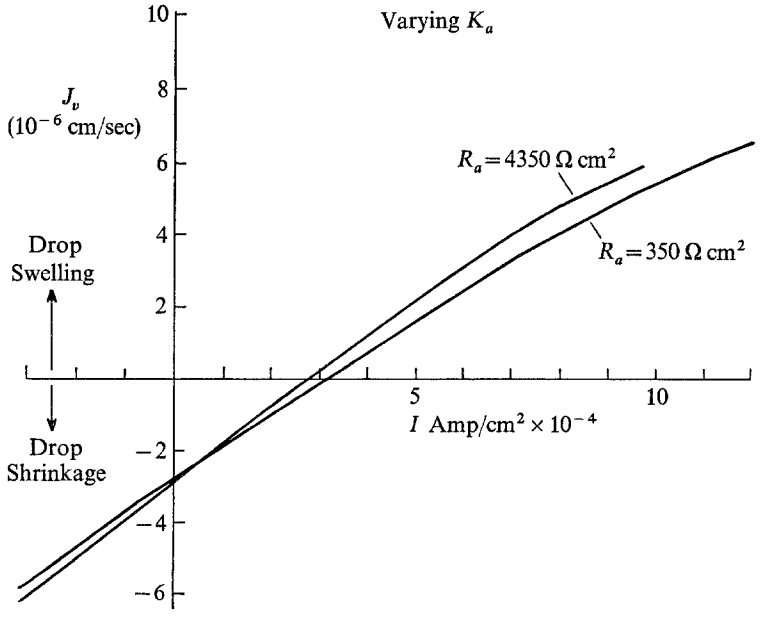

Fig. 4. (Left) J_v on ordinate, I on abscissa for limiting values of luminal membrane where luminal membrane solute per-

Fivefold variation of luminal membrane hydraulic conductivity, Lp_a, or wide variation of luminal membrane transference number difference, t_D^a, did not influence J_v, J_s or E. In Fig. 4 (left) a 10-fold variation in luminal membrane electrical conductance κ_a has almost no influence on J_v. However, changes in luminal membrane electrical conductance which reflect or are coincident with changes in luminal membrane permeability ω_a have a marked effect on volume flow (Fig. 4, right). A reduction of κ_a and ω_a in parallel results in a decreased passive NaCl influx into the tubule cell and therefore reduced active transport into the shunt path.

The properties of the shunt are the major determinants of the overall characteristics of the epithelium. Fig. 5 (left) shows the effect on J_v of small changes in the slit width of the tight junction (20 to 50 Å). Such small changes cause alterations in the cross-sectional area, NaCl permeability, conductance and hydraulic conductivity of the tight junction but were not assumed to significantly change its reflection coefficient. In Fig. 5 (right) the transference number of the tight junction was varied over a small range and an alteration in J_v occurred. Fig. 6 shows how changes in the total solute conductance of the shunt path influence the rate of fluid movement. These alterations were

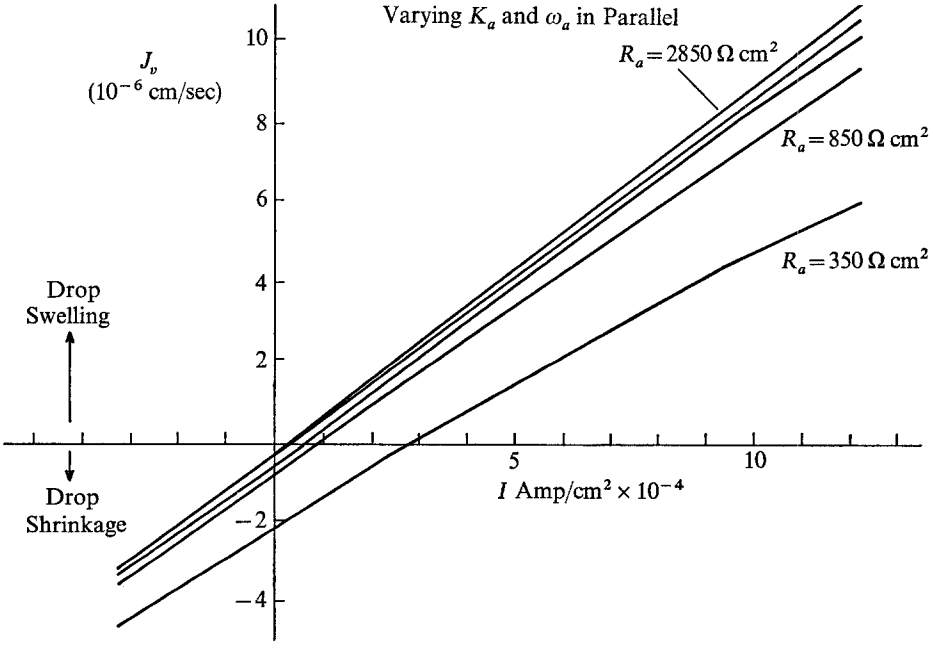

resistance. (Right) J_v *vs.* I, for 500 Ω cm^2 steps of luminal membrane resistance (R_a) meability (ω_a) changes proportionally

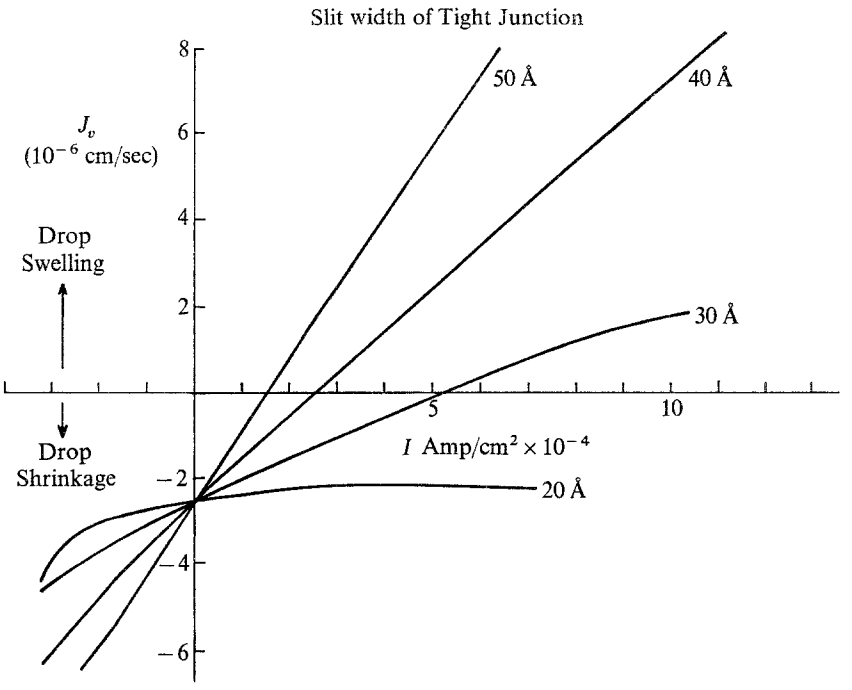

Fig. 5. (Left) J_v *vs.* I for various values of tight junction slit width.

achieved by variation in the lateral space-basement membrane conductance while tight junctional permeability remain unchanged. A widening of the lateral intercellular spaces, such as that observed during isotonic volume expansion, would be expected to result in reduced net fluid movement as a result of increased total solute conductance as shown here.

As shown in Fig. 1, the total epithelial electrical conductance κ, which is primarily a measure of shunt conductance, may increase during hyperpolarization of the tubule lumen. Fig. 7 shows the influence on J_v of changes in $1/\kappa$ from 86 Ω cm^2 to 21 Ω cm^2. Fig. 8 compares the J_v predicted by the model as a function of the command potential, E, with the experimentally observed values under voltage clamp. Since resistance decreases during hyperpolarizing commands, a line is included for the predicted effect of a decrease in transepithelial resistance from 55 Ω cm^2 to 25 Ω cm^2 at current densities greater than 3.2×10^{-4} amp/cm^2 (equivalent to a PD of 15 mV).

Table 4 lists the range of parameter estimates and flows observed in fitting 26 individual current clamp experiments. Table 5 lists the ratios of observed/predicted flows and forces for current clamp experiments. The model successfully reproduces the steady-state experimental observations of total PD, current density, and volume flow when supplied only with the

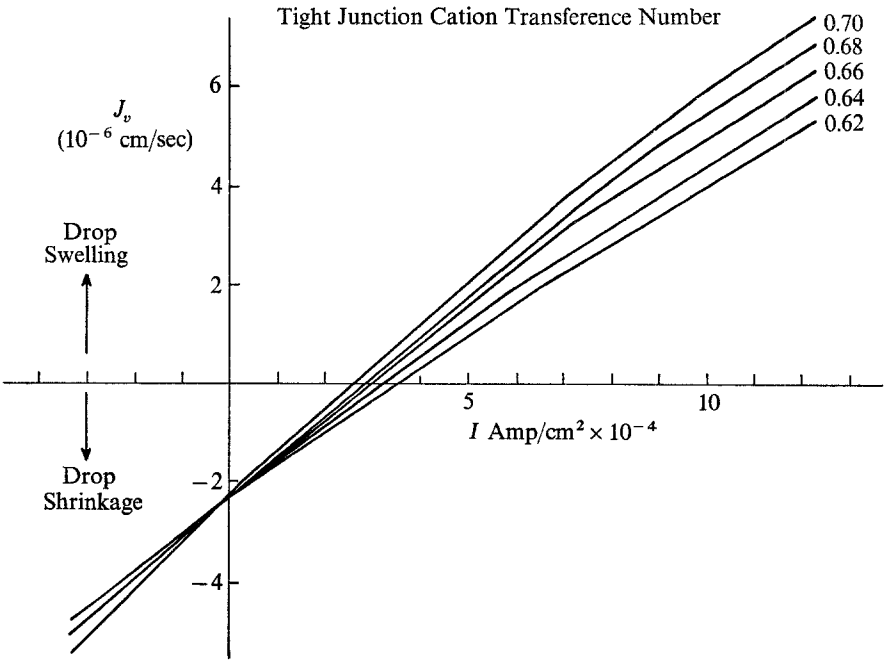

(Right) J_v *vs.* I for various values of tight junction cation transference number

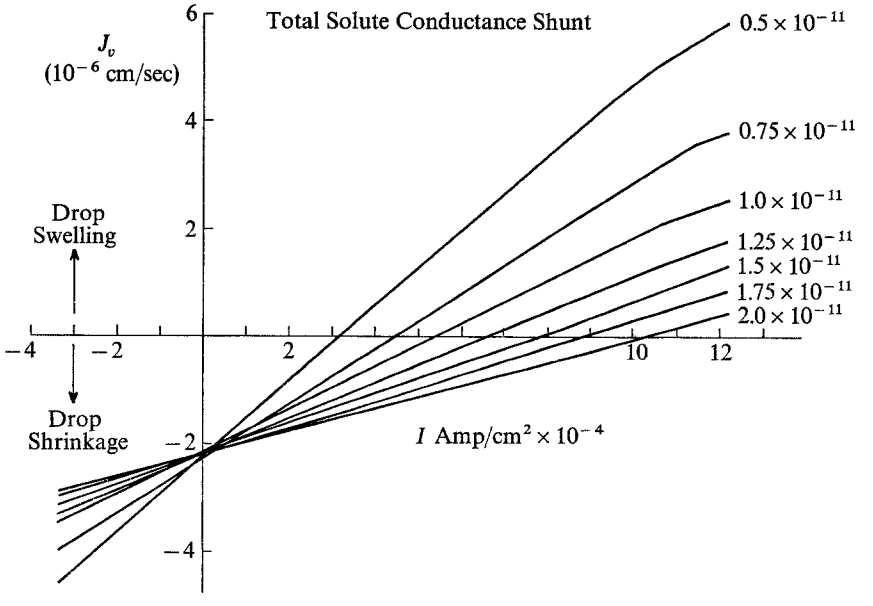

Fig. 6. J_v *vs.* I as function of variations in total shunt solute permeability (in moles/dyne sec)

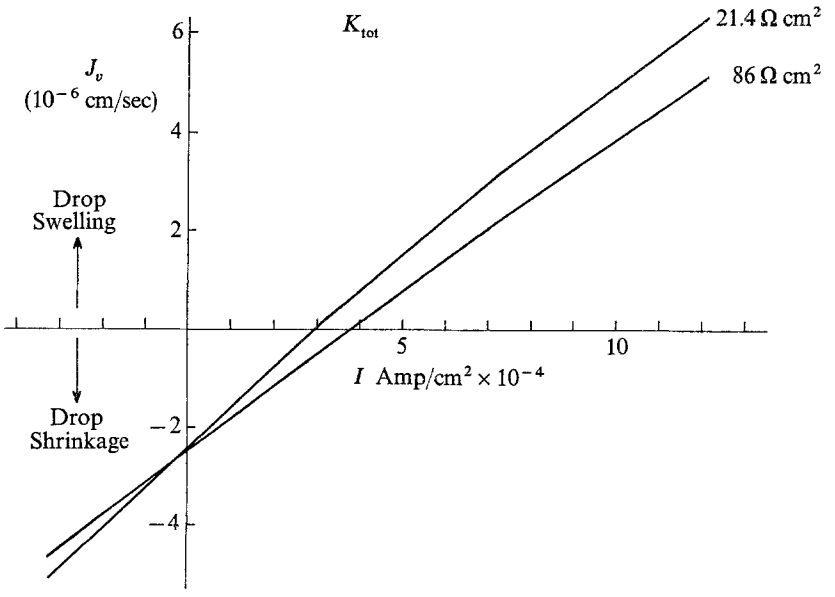

Fig. 7. J_v *vs.* I for the nominal range of total epithelial electrical resistance

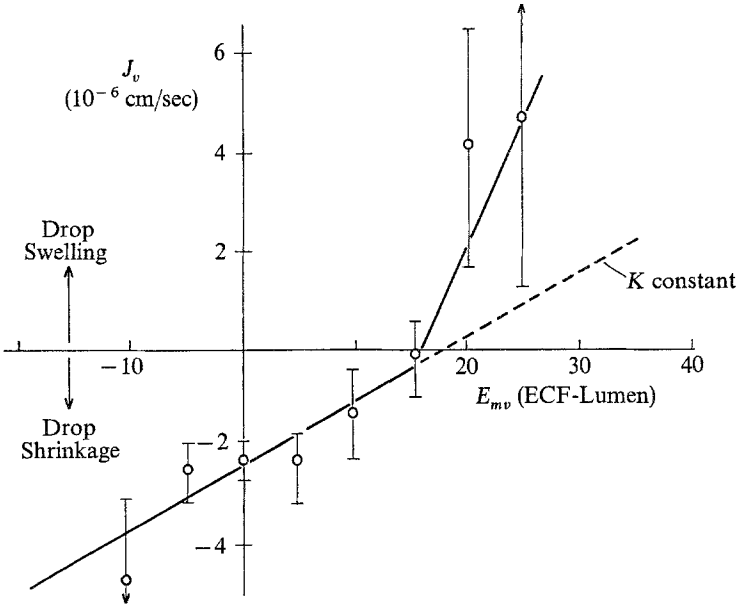

Fig. 8. J_v *vs* E, the command potential, during a voltage clamp for two cases: R constant at 55 Ω cm² and R decreases to 25 Ω cm² at E equal to 15 mV (lumen negative). Points are experimentally determined volume flows with one standard deviation range indicated

Table 4. Ranges of parameter and flow estimates during current clamps

Parameter[a]	Range
t_{Na} (epithelial Na transference number)	0.387→0.539
ω_s (epithelial solute permeability)	0.87→1.36 × 10^{-16} mole/dyne sec
α_b (fraction of electric current through shunt path) [b]	0.42→0.994
I (epithelial current density)	−1.15→3.68 mAmp/cm^2
J_v (volume flow)	−0.331→0.172 × 10^{-5} cm/sec
ΔC_s (change in NaCl conc. in interspace)	−32.8→24.0 mM/liter

[a] All other parameters constant at values in Tables 1–3.
[b] Cell specific resistance constant at 350 Ω cm^2 in all above calculations.

Table 5. Comparison of model predictions with experimental observations during current clamp

Steady-state variable	No. of obs.	Ratio $\frac{\text{observed}}{\text{theoretical}}$	t_{test} [a]
Total potential difference (E_{tot})	25	1.01 ± 0.09	n.s.
Spontaneous potential difference (E_{spon})	23	1.40 ± 0.13	$p<0.01$
Current density (I)	26	1.07 ± 0.26	n.s.
Volume flow (J_v)	17	1.23 ± 0.22	n.s.

[a] t test for significance of difference of ratio from 1.

initial values of spontaneous PD, electric current and a continuous record of transepithelial resistance. Spontaneous PD transients were slightly underestimated by the theory but this represents only a small difference in the magnitude of these transients and is explained to some extent by the use of average rate constants rather than the individual values.

Discussion

This model introduces and develops two new concepts of renal tubular epithelium: first, formal representation of the epithelium as a parallel path system, and secondly the consideration of the shunt path as a series of bar-

riers with different permeability characteristics. Epithelial parameters are seen to be predominantly determined by the shunt path properties. Additional conclusions may be summarized as follows: 1) most of the applied electric current flows through the shunt; 2) there is a difference between tight junction transference numbers and those of free solution and small changes in that difference may greatly influence J_v; 3) the lateral space dimensions strongly affect the overall permeability and conductivity of the shunt; 4) volume flows induced by current passage are the result of salt accumulation or depletion in the lateral spaces; 5) the magnitude of the voltage transients during and after current passage depends not only on the transference numbers of the tight junction but also on the transference properties of the lateral space and basement membrane; 6) most of the fluid flows across the tight junction; 7) most of the salt flows through the cells in the absence of applied current; 8) once salt has circumvented the tight junction it is not reflected by the remainder of the shunt path; 9) salt dilution potential experiments may not give direct information about the tight junction transference numbers because of the overwhelming influence of the lateral spaces under the experimental conditions. It is also worthy of note that none of the calculated shunt path parameters are physically or biologically unreasonable. It was not necessary to suggest aberrant physico-chemical behavior to duplicate the observed properties of the epithelium.

There are several important differences between this parallel path model and the simpler, single barrier representation of the epithelium. The parallel system admits, and in fact, necessitates circular internal flows of electric current and solute. An electric current loop which includes the cell and shunt path is responsible for a significant portion of the back leak of salt into the tubule lumen. Short-circuiting [35] would be expected to eliminate this current by an opposing current from external electrodes. It is also apparent that the back leak of salt into the lumen, caused by elevation of the salt concentration of the internal compartment of the shunt, is not influenced by short-circuiting. Since short-circuiting increases J_v, solvent drag effects nearly double. The active transport rate based on volume flows during short-circuit then underestimates the true rate by the difference between diffusion and solvent drag, about 10%. In the parallel path model, the passage of electric current creates NaCl concentration changes by the transport number effect [4] across the tight junction since this is the only site of discontinuity in transference numbers from free solution. If the properties of the entire epithelium were lumped and represented as a single barrier, the volume flows predicted by the transport number effect would disagree with the experimental results. From the overall transference number data of Boulpaep ($t_{Na}=0.4$,

$t_{Cl}=0.6$), no salt would be accumulated at the solution-membrane interfaces during current passage and there would be no J_v since there is not a significant transport number discontinuity. If the transference numbers estimated from conductances are used ($t_{Na}=0.25$, $t_{Cl}=0.75$ [1]) salt would be expected to accumulate at the anodic membrane-solution interface. This would result in a volume flow toward the anode while the experimental flow is observed to be toward the cathode. These discrepancies point to the need for the adoption of a distributed parameter model of the epithelium, since the biological implications of the experimental results differ depending on the model chosen.

Under some special circumstances the parallel path model may be approximated by a single barrier representation of the tubular epithelium. Expanding droplet experiments which involve large salt gradients across the epithelium and presumed reductions in the active transport rate to a very low level, are adequately depicted by a single barrier model [9, 13]. This representation seems only to be adequate when influx of NaCl into the tubule lumen from the ECF greatly overshadows any other transport phenomena in the epithelium. The single barrier model does not work as well in the absence of a salt gradient [9] and is not sufficiently complex to account for the effects of electric current passage.

The quantitative estimates of the properties of the shunt path which arise from the application of the parallel path equations give us additional insight into the probable patterns of salt and water movement. The hydraulic conductivity of the shunt, after correction for its small cross-sectional area, results in the prediction that most of the transported fluid passes through the tight junction rather than transcellularly. The parallel path model agrees with the proposals of others [8, 16, 17, 36, 38] that the principle route for salt movement out of the tubule lumen is transcellular, while back flux is predominantly extracellular. Essentially separate paths for ion and water movements have been previously proposed [15, 38, 44] but never quantitated as in the present work. The pattern of fluid and ion movement suggested here for *Necturus* tubule does not agree completely with that proposed for the rabbit gallbladder epithelium [36]. The electrical resistance changes [32, 43] which accompany osmotically induced water flows in *Necturus* proximal tubule are opposite those seen in gallbladder indicating possible differences between the two epithelia. However, the hydraulic conductivity data from which the path for water movement in proximal tubule is deduced come from two different laboratories and additional experiments are needed to confirm these results.

Representation of the shunt path as a series of barriers enables a quantitation of the relative importance of alterations in the geometry of the lateral

spaces and tight junction. Bentzel and coworkers [5, 6, 8] suggested that isotonic volume expansion may alter shunt permeability by changing tight junction and/or the effective linear path length from lumen to ECF. Boulpaep [13] proposed on the basis of electrophysiological and kinetic data that the lateral intercellular spaces widened during volume expansion leading to increased electrolyte and nonelectrolyte permeability. Alterations in tight junctional morphology were proposed as the basis for electrical conductance changes during the perfusion of anisotonic solutions [43]. Frömter [18] noted a correspondence between optically determined interspace width and electrical resistance of the *Necturus* gallbladder. The present calculations show that the tight junction contributes about one-fifth of the total solute and electrical resistance in the control *Necturus* proximal tubule (Table 2) when it is assumed that the NaCl diffusion coefficient is identical in both the tight junction and lateral intercellular spaces.

An adequate mathematical representation of the intercellular spaces as distensible structures requires knowledge of the forces which influence their degree of swelling. The observations of the previous paper suggest that the lateral spaces do not behave as osmometers, for when the salt concentration within the epithelium falls the spaces apparently swell. This conclusion is substantiated by several observations: hyperpolarizing commands cause volume flow into the lumen, decreased electrical resistance and increased solute conductance. The inward volume flow is the result of a lower salt concentration within the epithelium than in the lumen, while the increased electrical and solute conductances are consistent with widening of the lateral spaces (Fig. 1). An osmotic pressure difference cannot exist between the lateral spaces and the extracellular fluid ($\sigma_{bm}=0$, $\sigma_{Lis}=0$), but must occur across the tight junction ($\sigma_{TJ}=0.667$) when the salt concentration within the spaces is changed. An experimental situation comparable to a current-induced decrease in the osmotic pressure within the lateral spaces may be an increase in luminal tonicity; hypertonicity of the luminal fluid resulted in a fall in transepithelial resistance and hypotonicity caused an increase in resistance [43]. These changes, it should be noted, are opposite in direction to those observed during alterations in tonicity of mucosal solutions bathing the rabbit gallbladder [32], but are in complete agreement with the model presented here.

The spaces appear then to be "reverse osmometers", swelling as their salt concentration falls, a situation incompatible with previous experiences in biological membranes. The absence of significant streaming potentials (E. L. Boulpaep, *unpublished observations*) suggests that there is insufficient fixed charge in the shunt pathways to result in the negative anomalous

osmosis seen in highly charged artificial membranes [23]. Small cell volume changes could result in significant distortions of intercellular space volume but no data are presently available. Recent experiments on the physiological influence of small changes in the capillary oncotic [42] or hydrostatic pressures [22] suggest that they significantly alter lateral space dimensions. The possibility of hydrostatic pressure control of lateral space volume cannot be evaluated until additional data are available on the correlation between changes in this physical force and epithelial morphology.

The resistance changes caused by current passage in proximal tubule were markedly asymmetric. Depolarizing commands failed to significantly alter transepithelial resistance in most experiments, although in a few cases resistance rose a small amount (about 25%) during current passage. Perfusion of hypotonic solutions in the tubule lumen is known to cause large increases in resistance [43] suggesting that the lateral spaces may be further narrowed by this maneuver. Depolarizing current passage does not then seem to be readily effective in collapsing the lateral spaces. A comparable situation exists in the rabbit gallbladder in which osmotic changes of resistance are asymmetric since it is possible only to decrease resistance below control values [32].

I have not included variations in luminal or extracellular NaCl concentration in the physical forces to be varied in model calculations. There are several reasons for this: 1) the concentration dependence of the system parameters is unknown; 2) as shown in the Appendix, the electromotive forces and apparent transference numbers become a function of the internal concentration profiles of the epithelium; 3) the kinetics of active Na transport have not been investigated in the *Necturus* proximal tubule. All of the above areas are in need of thorough experimental investigation.

The most important value of a new model system is its influence on the design and interpretation of future experiments. Some additional considerations in the design of future experiments include: 1) the long relaxation time for intraepithelial concentration changes; 2) the high current density in the tight junction region of the shunt path (as much as 1 amp/cm^2 of tight junction); 3) the influence of imposed concentration changes on concentration-dependent parameter values such as solute permeability and transference number; 4) the important role of lateral intercellular space geometry in determining overall epithelial properties; 5) the possibilities of internal circulation of electric current and solutes; 6) the complicating influence of intraepithelial concentration profiles on determinations of transference numbers.

It is possible to use the model to predict the results of future experiments, such as: 1) NaCl reflection coefficients measured in a true "steady-state" should be considerably lower than the values determined instantaneously; 2) transference numbers measured during different degrees of distension of the lateral spaces should differ; e.g., as the spaces widen, the transference numbers determined by salt dilution potentials should approach those of the tight junction; 3) ion substitution should result in significant alterations in the rate of volume flow produced by a given current density; e.g., salt solutions in which transference numbers of cation and anion are similar (NaF, KCl) should show little or no fluid movement upon current passage. Finally, the model points out areas needing further investigation: 1) the concentration dependence of active Na transport; 2) the influence of current passage on intracellular composition; 3) the effects of concentration changes on permeability, conductance and transference numbers; 4) the factors which determine intercellular space distension; and 5) the potential dependence of the epithelial parameters.

Appendix

The purpose of this Appendix is the derivation of an expression for the electromotive force E as a function of the transference numbers and concentrations along the shunt pathway.

Consider the shunt path as two permeability barriers (tight junction *TJ* and lateral intercellular spaces *Lis*) separated by a thin layer of solution of indefinite volume.

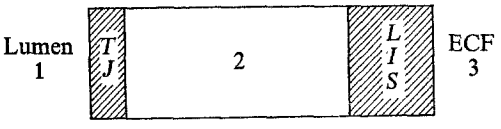

The total electromotive force is given by:

$$E = E_{TJ} + E_{Lis},$$

where

$$E_{TJ} = E_2 - E_1$$

and

$$E_{Lis} = E_3 - E_2.$$

In the steady-state, with $I=0$ and $J_v=0$, Eq. (1) reduces to:

$$-E = \frac{t^+_{TJ}\,\Delta\pi_s^{TJ}}{\nu z F \bar{C}_s^{TJ}} + \frac{t^+_{Lis}\,\Delta\pi_s^{Lis}}{\nu z F \bar{C}_s^{Lis}}, \tag{A.1}$$

where t_{TJ}^{+} and t_{Lis}^{+} are the cation transference numbers in each barrier, respectively, (assuming chloride reversible measuring electrodes). $\Delta\pi_s^{TJ}$ and $\Delta\pi_s^{Lis}$ are the osmotic pressure differences across *TJ* and *Lis*, respectively. $\bar{C}_s^{TJ}$ and $\bar{C}_s^{Lis}$ are the average concentrations across each barrier equal to:

$$\bar{C}_s^{TJ}=\frac{C^2-C^1}{\ln C^2/C^1},\qquad \bar{C}_s^{Lis}=\frac{C^3-C^2}{\ln C^3/C^2}. \tag{A.2}$$

Conservation of mass requires that:

$$\omega\Delta\pi_s=\omega_{TJ}\Delta\pi_s^{TJ}=\omega_{Lis}\Delta\pi_s^{Lis},$$

where ω is the total permeability of the path and ω_{TJ} and ω_{Lis} are the permeabilities of tight junction and lateral spaces, respectively.

$$\therefore\Delta\pi_s^{TJ}=\frac{\omega\Delta\pi_s}{\omega_{TJ}},\qquad \Delta\pi_s^{Lis}=\frac{\omega\Delta\pi_s}{\omega_{Lis}}. \tag{A.3}$$

Substituting Eq. (A3) into Eq. (A1) gives:

$$-E=\frac{t_{TJ}^{+}\omega\Delta\pi_s}{\nu zF\bar{C}_s^{TJ}\omega_{TJ}}+\frac{t_{Lis}^{+}\omega\Delta\pi_s}{\nu zF\bar{C}_s^{Lis}\omega_{Lis}},$$

or

$$-E=\frac{\omega\Delta\pi_s}{\nu zF}\left[\frac{t_{TJ}^{+}}{\bar{C}_s^{TJ}\omega_{TJ}}+\frac{t_{Lis}^{+}}{\bar{C}_s^{Lis}\omega_{Lis}}\right]. \tag{A.4}$$

Substituting Eq. (A2) into Eq. (A4) results in

$$-E=\frac{\omega\Delta\pi_s}{\nu zF}\left[\frac{t_{TJ}^{+}\ln C^2/C^1}{\omega_{TJ}(C^2-C^1)}+\frac{t_{Lis}^{+}\ln C^3/C^2}{\omega_{Lis}(C^3-C^2)}\right], \tag{A.5}$$

since $\Delta\pi_s=RT(C^3-C^1)$,

$$-E=\frac{RT\omega(C^3-C^1)}{\nu zF}\left[\frac{t_{TJ}^{+}\ln C^2/C^1}{\omega_{TJ}(C^2-C^1)}+\frac{t_{Lis}^{+}\ln C^3/C^2}{\omega_{Lis}(C^3-C^2)}\right]. \tag{A.6}$$

Eq. (A6) may be simplified by the relation

$$\omega(C^3-C^1)=\omega_{TJ}(C^2-C^1)=\omega_{Lis}(C^3-C^2)$$

to

$$-E=\frac{RT}{\nu zF}[t_{TJ}^{+}\ln C^2/C^1+t_{Lis}^{+}\ln C^3/C^2]. \tag{A.7}$$

When $C^1 = C^3$, Eq. (A7) simplifies to:

$$E = \frac{RT}{\nu z F}(t^+_{Lis} - t^+_{TJ}) \ln C^2/C^3. \tag{A.8}$$

For nonreversible electrodes, Eq. (A8) becomes:

$$E = \frac{RT}{\nu z F}(t^{Lis}_D - t^{TJ}_D) \ln C^2/C^3, \tag{A.9}$$

where $t_D = (t^+ - t^-)$.

In Eq. (A9) elevation of the concentration of the internal compartment, 2, causes a PD across two barriers. These EMF's may sum or oppose each other depending on their respective transference number differences.

In the case of an imposed salt gradient for the measurement of E to evaluate transference numbers, Eq. (A7) cannot be reduced to simpler form. The observed PD results then from the addition of two EMF's in series whose values depend directly on the magnitude of the individual concentration gradient across them as well as their transference numbers.

When Eq. (A7) is applied to the proximal tubule, the second barrier *Lis* is in reality a long, unstirred layer of solution. Only if the epithelium were a single barrier with well-stirred solutions on either side could Eq. (A7) be reduced to the Nernst-Planck-Henderson equation utilized by Frömter *et al.* [20].

The author thanks Drs. G. Giebisch and E. L. Boulpaep for many worthwhile discussions. Some of the concepts about hydrostatic pressure drops grew out of discussions with Dr. D. Marsh. Support is acknowledged from NIH training grant No. PHS AM 05644.

References

1. Anagnostopoulos, T. 1971. Evidence for independent Na and Cl transport pathways in *Necturus* kidney. *Abst. Amer. Soc. Nephrol.* p. 3
2. Asterita, M. F. 1971. Electrophysiological estimate of relative thickness of peritubular interstitial space in *Necturus* kidney. *Abst. Amer. Soc. Nephrol.* p. 5
3. Barry, P. H., Diamond, J. M. 1971. A theory of ion permeation through membranes with fixed neutral sites. J. Membrane Biol. **4**:295
4. Barry, P. H., Hope, A. B. 1969. Electroosmosis in membranes: Effects of unstirred layers and transport numbers. I. Theory. *Biophys. J.* **9**:700
5. Bentzel, C. J. 1971. Proximal tubular structure-function relationship during volume expansion in *Necturus* kidney. *Abst. Amer. Soc. Nephrol.* p. 9
6. Bentzel, C. J., Anagnostopoulos, T., Pandit, H. 1970. *Necturus* kidney: Its response to effects of isotonic volume expansion. *Amer. J. Physiol.* **218**:205
7. Bentzel, C. J., Davies, M., Scott, W. N., Zatzman, M., Solomon, A. K. 1968. Osmotic volume flow in the proximal tubule of *Necturus* kidney. *J. Gen. Physiol.* **51**:517

8. Bentzel, C. J., Parsa, B., Hare, D. K. 1969. Osmotic flow across proximal tubule of *Necturus:* Correlation of physiologic and anatomic studies. *Amer. J. Physiol.* **217**:570
9. Bentzel, C. J., Spring, K. R., Hare, D., Paganelli, C. V. 1973. Analog computer simulation of active and passive NaCl fluxes in *Necturus* proximal tubule. *Amer. J. Physiol.* (*In press*)
10. Bentzel, C. J., Tourville, D. R., Parsa, B. 1971. Bidirectional transport of horseradish peroxidase in proximal tubule of *Necturus* kidney. *J. Cell Biol.* **48**:197
11. Boulpaep, E. L. 1967. Ion permeability of the peritubular and luminal membrane of the renal tubule cell. *In:* Symposium über Transport und Funktion intracellulär Elektrolyte. F. Krück, editor. p. 98. Urban and Schwanzenberg, Berlin
12. Boulpaep, E. L. 1971. Electrophysiological properties of the proximal tubule: Importance of cellular and intercellular pathways. *In:* Electrophysiology of Epithelial Cells. G. Giebisch, editor. p. 91 F. K. Schattauer Verlag, Stuttgart
13. Boulpaep, E. L. 1972. Permeability changes of the proximal tubule of *Necturus* during saline loading. *Amer. J. Physiol.* **222**:517
14. Clarkson, T. W. 1967. The transport of salt and water across isolated rat ileum. *J. Gen. Physiol.* **50**:695
15. Claude, P. 1968. An Electron Microscopic Study of the Urinary Tubules of *Necturus* Maculosus. Ph. D. Thesis. University of Pennsylvania, Philadelphia, Pa.
16. Diamond, J. M., Barry, P. H., Wright, E. M. 1971. The route of transepithelial ion permeation in the gall bladder. *In:* Electrophysiology of Epithelial Cells. G. Giebisch, editor. p. 23. F. K. Schattauer Verlag, Stuttgart
17. Diamond, J. M., Bossert, W. H. 1967. Standing-gradient osmotic flow. *J. Gen. Physiol.* **50**:2061
18. Frömter, E. F. 1972. The route of passive ion movement through the epithelium of *Necturus* gall bladder. *J. Membrane Biol.* **8**:259
19. Frömter, E. F., Diamond, J. M. 1972. Route of passive ion permeation in epithelia. *Nature, New Biol.* **235**:9
20. Frömter, E. F., Müller, C. W., Wick, T. 1971. Permeability properties of proximal tubular epithelium of the rat kidney as studied with electrophysiological methods. *In:* Electrophysiology of Epithelial Cells. G. Giebisch, editor. p. 119. F. K. Schattauer Verlag, Stuttgart
21. Giebisch, G. 1969. Functional organization of proximal and distal tubular electrolyte transport. *Nephron* **6**:260
22. Grandchamp, A., Boulpaep, E. L. 1972. Effect of intraluminal pressure on proximal tubular sodium reabsorption. A shrinking drop micropuncture study. *Yale J. Biol. Med.* **45**:275
23. Grim, E., Sollner, K. 1957. The contributions of normal and anomalous osmosis to the osmotic effects arising across charged membranes with solutions of electrolytes. *J. Gen. Physiol.* **40**:887
24. Hoshiko, T., Lindley, B. D. 1967. Phenomenological description of active transport of salt and water. *J. Gen. Physiol.* **50**:729
25. Jacquez, J. A., Carnahan, B., Abbrecht, P., 1967. A model of the renal cortex and medulla. *Math. Biosci.* **1**:227
26. Katchalsky, A. 1968. Thermodynamic treatment of membrane transport. *Pure Appl. Chem.* **16**:229
27. Kedem, O., Katchalsky, A. 1961. A physical interpretation of the phenomenological coefficients of membrane permeability. *J. Gen. Physiol.* **45**:143
28. Kedem, O., Katchalsky, A. 1963. Permeability of composite membranes. *Trans. Faraday Soc.* **59**:1918
29. Mandel, L. J., Curran, P. F. 1972. Responses of frog skin to steady-state voltage clamping. *J. Gen. Physiol.* **59**:503

30. Oken, D. E., Whittembury, G., Windhager, E. E., Solomon, A. K. 1963. Single proximal tubules of *Necturus* kidney. V. Unidirectional sodium movement. *Amer. J. Physiol.* **204**:372
31. Rose, R. C., Schultz, S. G. 1971. Studies on the electrical potential profile across rabbit ileum. *J. Gen. Physiol.* **57**:639
32. Smulders, A. P., Tormey, J. McD., Wright, E. M. 1972. The effect of osmotically induced water flows on the permeability and ultrastructure of the rabbit gallbladder. *J. Membrane Biol.* **7**:164
33. Solomon, A. K. 1963. Single proximal tubules of *Necturus* kidney. VII. Ion fluxes across individual faces of cell. *Amer. J. Physiol.* **204**:381
34. Spring, K. R. 1973. Current-induced voltage transients in *Necturus* proximal tubule. *J. Membrane Biol.* **13**:299
35. Spring, K. R., Paganelli, C. V. 1972. Sodium flux in *Necturus* proximal tubule under voltage clamp. *J. Gen. Physiol.* **60**:181
36. Tormey, J. M., Diamond, J. M. 1967. The ultrastructural route of fluid transport in rabbit gall bladder. *J. Gen. Physiol.* **50**:2031
37. Welling, L. W., Grantham, J. J. 1972. Physical properties of isolated perfused renal tubules and tubular basement membranes. *J. Clin. Invest.* **51**:1063
38. Whittembury, G. 1967. Sobre los mecanismos de absorción en el tubo proximal del riñón. *Acta Cient. Venezolana Suppl.* I. **3**:71
39. Whittembury, G., Oken, D. E., Windhager, E. E., Solomon, A. K. 1959. Single proximal tubules of *Necturus* kidney. IV. Dependence of H_2O movement on osmotic gradients. *Amer. J. Physiol.* **197**:1121
40. Whittembury, G., Sugino, N., Solomon, A. K. 1960. Effect of anti-diuretic hormone and calcium on the equivalent pore radius of kidney slices from *Necturus*. *Nature* **187**:699
41. Whittembury, G., Sugino, N., Solomon, A. K. 1961. Ionic permeability and electrical potential differences in *Necturus* kidney cells. *J. Gen. Physiol.* **44**:689
42. Windhager, E. E. 1968. Glomerulo-tubular balance of salt and water. *Physiologist* **2**:103
43. Windhager, E. E., Boulpaep, E. L., Giebisch, G. 1967. Electrophysiological studies on single nephrons. *In:* Proceedings of the International Congress of Nephrology, Volume I: Physiology. J. S. Handler, editor. p. 35. S. Karger, Basel
44. Windhager, E. E., Giebisch, G. 1965. Electrophysiology of the nephron. *Physiol. Rev.* **45**:214
45. Wright, E. M., Smulders, A. P., Tormey, J. McD. 1972. The role of the lateral intercellular spaces and solute polarization effects in the passive flow of water across the rabbit gallbladder. *J. Membrane Biol.* **7**:198